Localized Coverage Planning for a Heat Transfer Tube Inspection Robot

Jiawei Li, Zhaojin Liu, Yuxiao Li, Yuanyue Li, *Graduate Student Member, IEEE*, Yimin Huang, and Gang Wang, *Senior Member, IEEE*

***Abstract*—The heat transfer tubes of the steam generator are critical components of the nuclear power system and require regular inspection to ensure safety. The SG-Climbot, a quadruped heat transfer tube inspection robot, is equipped with a guiding device capable of simultaneously aligning with and inspecting two heat transfer tubes. Furthermore, The guiding device must execute hundreds of pose configuration transformations to complete a localized coverage inspection, thereby presenting challenges to the robot's efficient autonomous planning. This letter presents a planning framework for the SG-Climbot's localized coverage inspection task. The framework consists of four planning levels: pair planning, position and orientation planning for the guiding device, inspection sequence planning, and time-optimal trajectory planning. A maximum matching algorithm suitable for robotic arms equipped with dual execution devices to perform tasks has been proposed, achieving the optimal pairing of heat transfer tubes and reducing inspection time by over 48 minutes (18.32% improvement). In addition, we analyze the impact of various Traveling Salesman Problem (TSP) solving algorithms on sequence planning issues that require reaching numerous nodes within short operation times, reducing the arm operating time by 33.20 s (6.99% improvement). Finally, the effectiveness of the proposed planning algorithm was validated through simulations and experiments.**

***Index Terms*—Task and motion planning, industrial robots, heat transfer tube inspection.**

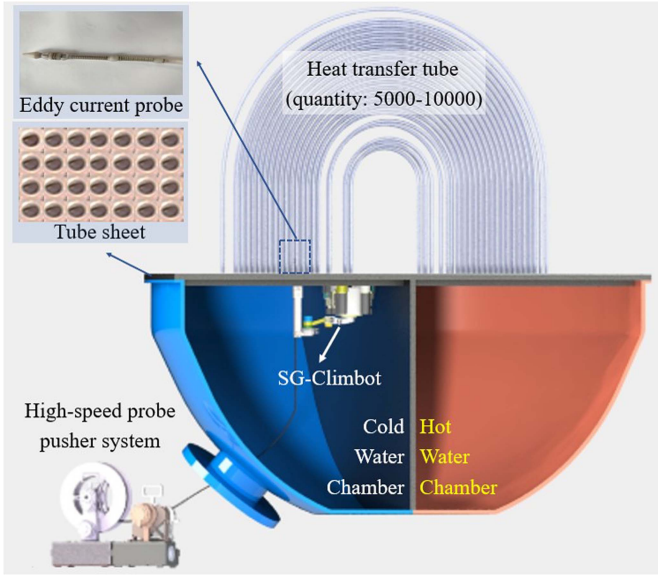

Fig. 1. Heat transfer tube inspection process.

I. Introduction

NUCLEAR energy is a clean, low-carbon, safe, and efficient energy source that plays a significant role in advancing global economic and social development [1]. The steam generator (SG), which connects the primary and secondary circuit systems within a nuclear power plant, is a vital component of nuclear safety. Its tube sheet and inverted U-shaped heat transfer tubes constitute integral parts of the primary circuit coolant pressure boundary. Regular inspections of the heat transfer tubes within the steam generator are essential for ensuring the safety of the nuclear power system [2]. The inspection process requires the deployment of a remotely controlled robot in the water chamber of the SG. Following installation, the robot must navigate to the designated location and rotate its inspection arm to align the guiding device with the heat transfer tube. Subsequently, the eddy-current probe is inserted into the U-shaped heat transfer tube using a high-speed probe pusher system to facilitate tube inspection [3], as illustrated in Fig. 1.

The SG-Climbot, as illustrated in Fig. 1, a quadruped robot designed for heat-transfer-tube inspection, demonstrates adaptability to various tube sheets, an extensive inspection range, high mobility, and effective inspection capabilities. The robot is mounted upside down on the tube sheet. The pneumatic tensioning mechanism carried by the feet of the robot is inserted into the heat transfer tube, tightening the tensioning mechanism to secure the robot to the tube sheet, as shown in Fig. 2. The crawling process of the robot begins with adjustments to the body position of the robot and the angle of its legs while maintaining its foothold position. Each leg undergoes a sequence of actions, including loosening and retracting the tensioning mechanism, swinging, extending and tightening the tensioning mechanism to complete one crawling cycle. More importantly, as the robot

Received 7 November 2024; accepted 20 February 2025. Date of publication 3 March 2025; date of current version 14 March 2025. This article was recommended for publication by Associate Editor Z. Wang and Editor H. Moon upon evaluation of the reviewers' comments. This work was supported by the National Key Research and Development Program of China under Grant 2023YFB3407702. *(Jiawei Li and Zhaojin Liu contributed equally to this work.) (Corresponding author: Gang Wang.)*

The authors are with the National Key Laboratory of Autonomous Marine Vehicle Technology, Harbin Engineering University, Harbin 150001, China (e-mail: ljw1996@hrbeu.edu.cn; liuzhaojin@hrbeu.edu.cn; liyuxiao@hrbeu.edu.cn; liyuanyue@hrbeu.edu.cn; hym0128@hrbeu.edu.cn; wanggang@hrbeu.edu.cn).

This article has supplementary downloadable material available at https://doi.org/10.1109/LRA.2025.3547675, provided by the authors.

Digital Object Identifier 10.1109/LRA.2025.3547675

IEEE Robotics and Automation Letters (RA-L) paper, presented at ICRA 2026, Vienna, Austria. Cite as RA-L paper.

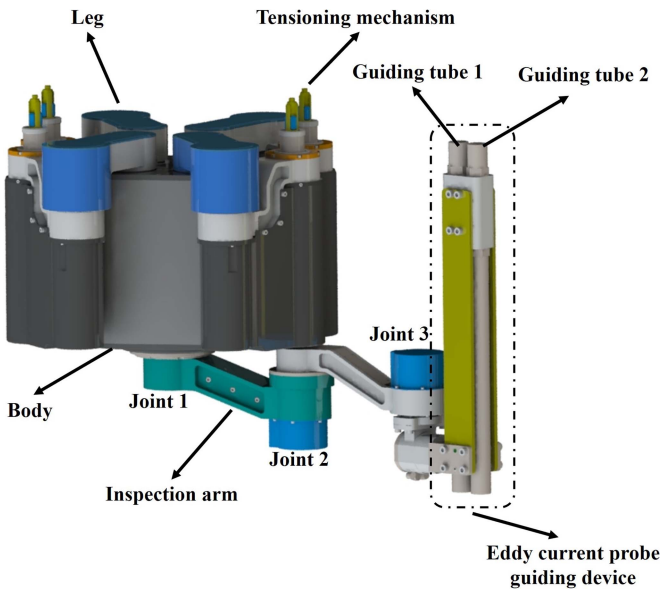

Fig. 2. Structure of SG-Climbot.

crawls within a specified range, the absolute position of a guiding device can remain constant. This feature significantly enhances the efficiency of the robot in executing complete coverage inspection tasks. The advantages and operational environment of the SG-Climbot have been detailed in previous research [7].

The localized coverage inspection discussed in this letter refers to the robot inspecting heat transfer tubes requiring inspection within its inspection range while the robot body remains stationary. Localized coverage inspection, as a subproblem of complete coverage inspection, is crucial for the maintenance cycle of SGs. The localized coverage inspection process is as follows: The robot can be suspended upside down on a tube sheet via a tensioning mechanism at its foot end. It then rotates the inspection arm to align the guiding device with the designated heat transfer tube. Subsequently, an eddy current probe is inserted into the heat transfer tube through a high-speed probe pusher system for an inspection duration of 1 to 2 minutes. The inspection arm subsequently rotates to align the guiding device with the next heat-transfer tube requiring inspection, continuing this procedure until all heat-transfer tubes within the specified range have been examined. The time for the eddy current probe to inspect the heat transfer tubes will be referred to as the "inspection time". Additionally, the operation time of the inspection arm (the execution time of its trajectory) will be referred to as the "operation time".

This letter investigates the localized coverage inspection planning for a quadruped heat transfer tube inspection robot, with the primary contributions as follows: (1) A novel planning framework is proposed for the localized coverage inspection of heat transfer tubes; (2) a maximum matching method is proposed under the constraints of the structure of the guiding device and the kinematics of the inspection arm. This method significantly reduces the time required to inspect heat tubes with an eddy current probe. It offers an effective solution for the coverage planning task of an inspection arm equipped with dual execution devices at the end; (3) we analyze the impact of various TSP-solving algorithms on sequence planning problems that involve reaching numerous nodes within short operation times, effectively enhancing the operational efficiency of inspection arms.

The remainder of this letter is organized as follows: We review the related literature in Section II. Section III details the robot structure, inverse kinematics, and inspection range. Section IV describes the planning framework and the methods employed at each planning level. Section V presents the effectiveness of the proposed planner based on simulation and experimental results. Finally, Section VI concludes the letter and proposes directions for future research.

II. Related Works

The problem we aim to address is related to coverage planning. Area coverage is essential for various robotic applications, such as agricultural field cultivation, lawn mowing, structural inspection, drone monitoring, robotic vacuum cleaning, etc [8], [9], [10], [11], [12]. These problems pertain to coverage planning for mobile robots; however, our focus is on solving the coverage planning issue for the end-effector of a manipulator. Currently, in the research on coverage planning for the end-effector of a manipulator, Ren et al. [13] proposed a management method for distributing the blasted areas using an editing program on irregular surfaces and improved the genetic algorithm to obtain an efficient sanding path for the robotic arm, with the objectives of minimizing travel distance and steering angle. Leidner et al. [14] introduced an approach for redundant robotic arms to accomplish cleaning operations. The wiping task's medium is characterized by generic particle distribution, and the motion planning bifurcates into a high-level planning module and specific controls for the requisite cleaning maneuvers. Yet, the authors concentrated on optimizing the Cartesian path length at the robotic arm's terminal end effector, neglecting the joint space expenses. Hess et al. [15] framed the surface coverage path planning for redundant robots as a Generalized Traveling Salesman Problem (GTSP), establishing that accounting for joint space costs outperforms Cartesian space cost functions in operational workload and task completion timelines. Kaljaca et al. [16] articulated the shrubbery trimming issue for manipulators equipped with trimming tools at their end effectors as a GTSP, utilizing a grid representation of the shrub's anticipated configuration, and incorporating a joint space cost function for manipulation posture to effectuate optimal node traversal sequencing. Zhang et al. [17] propose a joint base placement and multi-configuration disinfected path planning (JPMDP) method, which fully considers the movement costs between multi-configuration to ensure the efficiency of the disinfection process. However, the method does not provide a detailed description of the time allocation for trajectory planning.

In current studies on coverage planning for robotic arms, the end effector is equipped with only one execution device, such as for spraying or disinfection tasks. The guiding device employed by the SG-Climbot consists of two guiding tubes, which can simultaneously inspect two heat transfer tubes. Successfully pairing an additional set of heat transfer tubes can reduce inspection time by approximately 1 to 2 minutes. There is a lack

IEEE Robotics and Automation Letters (RA-L) paper, presented at ICRA 2026, Vienna, Austria. Cite as RA-L paper.

of research in the literature on maximum matching problems under constraints such as the structure of the guiding device and the kinematics of the inspection arm. Algorithms related to maximum matching numbers, such as the Hungarian algorithm [18] and the Hopcroft-Carp algorithm [19], which are employed to solve matching problems in bipartite graphs (two disjoint subsets), cannot be applied to the optimal pairing problem of heat transfer tubes. In practical engineering, a column-pairing method is often used. However, in cases where the inspection range is irregular or randomly sampled, obtaining the optimal pairing solution is difficult, greatly increasing the inspection time. Moreover, coverage sequence planning for robotic arms is frequently modeled as a Traveling Salesman Problem (TSP). The requirement to solve the TSP before commencing the operation of the inspection arm means that the algorithm's running time directly influences the overall efficiency of the coverage task. Particularly in scenarios discussed in this letter, where operation times are brief yet many nodes must be accessed, employing TSP-solving algorithms with high time complexity significantly reduces task completion efficiency. We took inspiration from these previous works and fully consider the characteristics of the localized coverage detection task for heat transfer tubes, proposing a novel localized coverage inspection planning framework. By addressing the maximum matching problem of heat transfer tubes and sequence planning issues that require reaching numerous nodes within short operation times, we improved the inspection efficiency of the robot.

III. SG-Climbot Overview

A. Structure of SG-Climbot

The design of the SG-Climbot, depicted in Fig. 2, features a planar, quadruped structure tailored for crawling on a tube sheet. A specialised tensioning mechanism at the foot end ensures stability while hanging upside down on the tube sheet during locomotion and inspection. The robot is equipped with a 3-DOF inspection arm, which has a guiding device with an eddy current probe at its end. The guiding device consists of two guiding tubes that can simultaneously align with two heat transfer tubes. A high-speed probe pusher system is used to insert the eddy-current probe into the U-shaped heat transfer tube to complete the inspection of the tubes.

B. Inspection Arm Inverse Kinematics

The inspection arm mounted on the SG-Climbot is a planar, 3-DOF arm, and the guiding device at its end must transition from the initial pose to the final pose within the workspace. Kinematics can determine joint angles, which necessitates knowledge of the control point coordinates (the center point of the two guiding tubes) and the angle ϕ_e of the guiding device, as illustrated in Fig. 3. The redundancy can be avoided by defining the angle of link 2 (θ_2) as positive, meaning counter-clockwise relative to link 1. The solution for the inverse kinematics of the inspection arm is presented as follows:

$$\theta_1 = \tan^{-1}\frac{yy}{xx} \pm \cos^{-1}\left(\frac{xx^2+yy^2+l_1^2-l_2^2}{2l_1\sqrt{xx^2+yy^2}}\right) \quad (1)$$

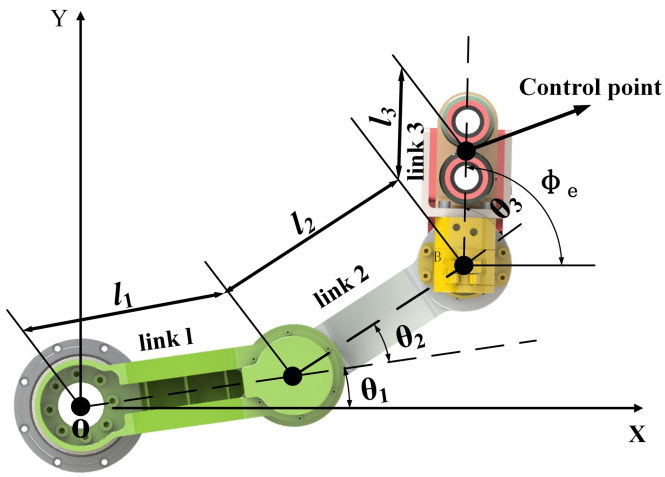

Fig. 3. Inspection arm.

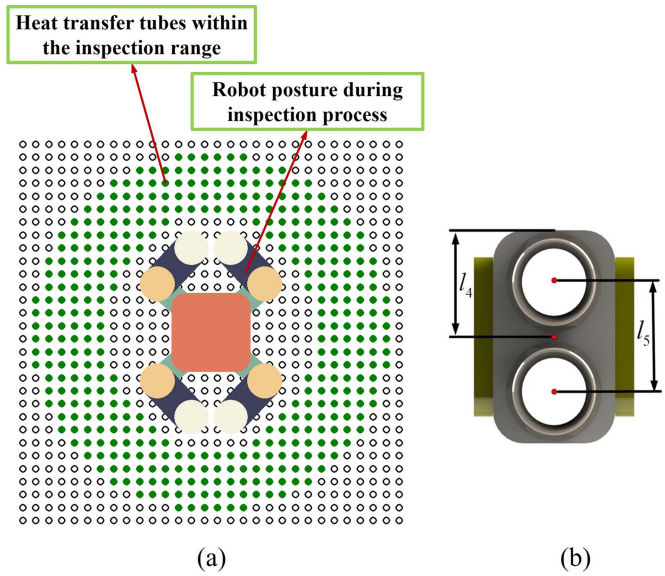

Fig. 4. Inspection range, robot posture, and top view of guiding device. (a) Inspection range and robot posture; (b) top view of guiding device.

$$\theta_2 = \pm\left(\pi - \cos^{-1}\left(\frac{l_1^2+l_2^2-xx^2-yy^2}{2l_1l_2}\right)\right) \quad (2)$$

$$\theta_3 = \phi_e - \theta_1 - \theta_2 \quad (3)$$

Where $xx = x - l_3\cos(\phi_e)$ and $yy = y - l_3\sin(\phi_e)$; l_1, l_2, l_3 represent the lengths of link 1, link 2, and link 3; (x, y) denotes the coordinates of the end control point; ϕ_e indicates the angle of the guiding device.

C. Inspection Range

Fig. 4(a) depicts the posture of the robot during inspection. In this study, the inspection range is defined as heat transfer tubes that can be inspected by the guiding device while the robot remains stationary. Initially, we calculate the union of the reachable spaces of guiding tube 1 and guiding tube 2 that satisfy the kinematic constraints of the inspection arm and the joint angle limitations. Due to occlusion caused by the body and legs

IEEE Robotics and Automation Letters (RA-L) paper, presented at ICRA 2026, Vienna, Austria. Cite as RA-L paper.

of the robot, it is necessary to remove the heat transfer tubes that fall within the projected area of the body and legs from the reachable spaces. To simplify subsequent obstacle avoidance strategies, we expand the projection of the robot's body and legs using the expansion length (l_4) shown in Fig. 4(b). As long as the control points on the guiding device do not fall within the projected area, the guiding device will not collide with the robot's body or legs, regardless of its posture. If the heat transfer tubes enclosed by the legs are inaccessible to the guiding device, those heat transfer tubes enclosed by the legs will also be eliminated. The remaining heat transfer tubes constitute the inspection range of the inspection arm. As shown in Fig. 4(a), the green dots represent the heat transfer tubes included in the inspection range.

IV. Planning Algorithm

This letter introduces an innovative planning framework for the localized coverage inspection task of the SG-Climbot. The framework encompasses four planning levels: pairing planning, position and orientation planning for the guiding device, inspection sequence planning, and time-optimal trajectory planning. By employing pairing planning and position and orientation planning for the guiding device, all the poses that the guiding device needs to reach can be obtained. Inspection sequence planning can establish the sequence for reaching all poses of the guiding device, while time-optimal trajectory planning yields the trajectory in the joint space of the inspection arm to achieve the inspection process.

A. Pairing Planning

The SG-Climbot, equipped with a guiding device capable of simultaneously inspecting two heat transfer tubes, necessitates the pairing of these tubes based on the distance between the guiding tubes and the constraints of the inspection arm. Successfully pairing even one additional set of heat transfer tubes can result in a savings of 1 to 2 minutes in inspection time. This letter presents a 0–1 integer programming method to address the heat transfer tube pairing problem and utilizes the implicit enumeration method to derive optimal pairings. The definition of the optimal pairing problem for heat transfer tubes is as follows:

Find:

$$\max \sum_{i<j}^{n} x_{ij} \tag{4}$$

Subject to:

$$x_{ij} = \begin{cases} 0,1 & d_{ij} = l_5 \;\&\; IK_{ij}\ solvable \\ 0 & \text{else} \end{cases} \tag{5}$$

$$\sum_{i=0}^{n} \left(\sum_{j=0}^{i} x_{ij} + \sum_{i+1}^{n} x_{ij} \right) \leq 1 \tag{6}$$

Establish a distance matrix $D^{n\times n}$, where n is the number of heat transfer tubes in the inspection range, the element d_{ij} in the distance matrix $D^{n\times n}$ represents the distance between the

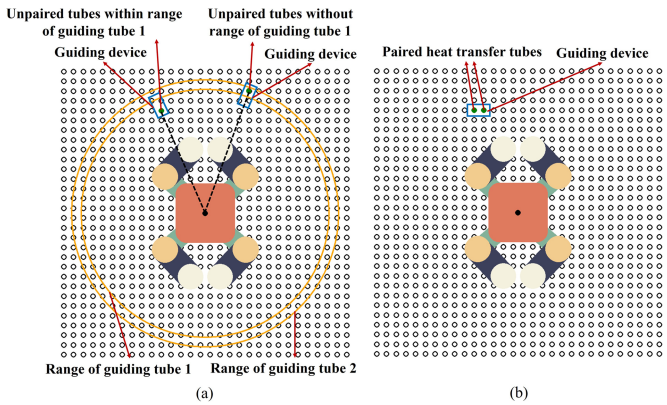

Fig. 5. Position and orientation of guiding device. (a) Position and orientation of guiding device for unpaired heat transfer tubes; (b) position and orientation of guiding device for paired heat transfer tubes.

*i*th and *j*th heat transfer tubes. Establish a pairing matrix $X^{n\times n}$, where x_{ij} is the element in the *i*th row and *j*th column of the pairing matrix, representing whether the *i*th and *j*th heat transfer tubes have been successfully paired. If the pairing is successful, $x_{ij} = 1$; if unsuccessful, $x_{ij} = 0$. l_5 represents the center distance between the two guiding tubes, as shown in Fig. 4(b). In formula (5), "$IK_{ij}\ solvable$" indicates that after pairing the *i*th and *j*th heat transfer tubes, incorporating the position and posture of the guiding device (as shown in Fig. 5(b)) into the inverse kinematics formulas in Section III-B results in a feasible solution. Formula (6) is designed to limit the numerical values of the elements in the pairing matrix to avoid repeated pairings of heat transfer tubes.

B. Position and Orientation Planning

If the heat transfer tubes are successfully paired, the positions and orientations of the guiding device during inspection can be readily obtained, as shown in Fig. 5(b). For heat transfer tubes that are not successfully paired, they are inspected with guiding tube 1; if they are outside the inspection range of guiding tube 1, then they are inspected with guiding tube 2. In both cases, the orientation of the guiding device is directed toward the center of the body, as illustrated in Fig. 5(a).

C. Inspection Sequence Planning

Sections IV-A and IV-B provide multiple positions and orientations that the guiding device must reach to complete the localized coverage inspection task. The objective of planning the inspection sequence is to minimize operational time while ensuring that the guiding device can reach all required positions and orientations. This problem is typically defined as TSP. We construct a graph G = (V, E), where V represents the set of nodes and E represents the set of edges, using the joint rotation angles as the cost function for generating the optimal inspection sequence [15].

The inverse kinematics discussed in Section III-B is employed to calculate the joint configurations of the guiding device as it reaches the specified position and orientation. Assume the

IEEE Robotics and Automation Letters (RA-L) paper, presented at ICRA 2026, Vienna, Austria. Cite as RA-L paper.

maximum joint velocity is $\nu_{\max}$, The movement cost between any two joint configurations is expressed in formula(7):

$$dist(p_i, p_j) = \begin{cases} \max\left(\frac{\|\Delta q_{ij}^m\|}{\nu_{\max}}\right) & \text{if no collisions} \\ \max\left(\frac{\|\Delta q_{ij}^m\|}{\nu_{\max}}\right) + h & \text{if has collisions} \end{cases} \tag{7}$$

p_i and p_j represent the *i*th and *j*th joint configurations, respectively; Δq_{ij}^m represents the angular change produced by the *m*th joint when moving between these two joint configurations. If there are obstacles between two joint configurations, additional path planning will incur extra costs, necessitating the addition of a high value h to the original cost. In this letter, obstacles refer to the legs and body of the robot, which may collide with the guiding device.

Solving the TSP is classified as NP-hard. The TSP associated with coverage planning is typically addressed using algorithms such as the nearest neighbor search algorithm, 2-opt, Lin-Kernighan-Helsgaun (LKH), and dynamic programming [16], [20], [21]. Since the inspection arm can execute inspection tasks only after the inspection sequence has been established, this study must consider both the operational time of the robotic arm and the algorithm's runtime for solving the TSP, as both significantly influence the efficiency of the robotic arm's coverage inspection. Given that the inspection sequence planning requires reaching up to 100–300 nodes, the computation times for the LKH and dynamic programming algorithms would greatly surpass the coverage inspection time of the inspection arm (no valid solution was obtained within 10 minutes). Thus, these algorithms are excluded from consideration in this study. This letter will compare the impacts of two algorithms with lower time complexity—the nearest neighbor search and 2-opt—on the efficiency of the robotic arm's coverage inspection, as demonstrated in the simulation presented in Section V-B.

D. Time-Optimal Trajectory Planning

In Section IV-C, the potential for collisions involving the guiding device during linear movements of the control point between different joint configurations has been effectively assessed. In the absence of collisions, the control point traverses a straight path. The orientation of the guiding device on the path is determined using uniform linear interpolation based on the initial orientation of the guiding device, the target orientation of the guiding device, and the movement distance of the control point. To ensure the continuity of joint velocity and acceleration, the path was discretized, and the joint angles were generated using inverse kinematics. Subsequently, cubic B-spline curves were employed to generate trajectories in the joint space of the inspection arm to effectively ensure the continuity of joint velocity and acceleration, and to facilitate the handling of velocity and acceleration constraints during the process of optimizing trajectory time.

The total time interval between each pair of waypoints in the spline curve determines the time required for the inspection arm to move between adjacent joint configurations. The objective of the trajectory planning in this letter is to minimize the time for the movement trajectory between adjacent joint configurations while satisfying the constraints of maximum joint velocity and acceleration. We model this problem as a nonlinear optimization problem, the time-optimal trajectory planning problem is defined as:

Find:

$$\min \sum_{i=1}^{\mathrm{n}-1} h_i \tag{8}$$

Subject to:

$$|\dot{q}_j(t)| \le V_j \quad j = 1, 2, 3 \tag{9}$$

$$|\ddot{q}_j(t)| \le W_j \quad j = 1, 2, 3 \tag{10}$$

$$h_i \ge \max\left(\frac{Q_{ij}}{V_j}\right) \quad j = 1, 2, 3 \tag{11}$$

In the formula, h_i represents the time interval from the *i*th waypoint to the (*i+1*)th waypoint; n denotes the number of waypoints; $q_j(t)$ indicates the angle of the *j*th joint at time t; $\dot{q}_j(t)$ indicates the angular velocity of the *j*th joint at time t; $\ddot{q}_j(t)$ indicates the angular acceleration of the *j*th joint at time t; V_j signifies the maximum angular velocity of the *j*th joint; W_j represents the maximum angular acceleration of the *j*th joint; and Q_{ij} indicates the angle that the *j*th joint needs to rotate during the *i*th time interval. The SLSQP function from the SciPy [23] library can be utilized to solve the aforementioned nonlinear optimization problem, yielding the time-optimal trajectory between adjacent joint configurations.

If the straight movement of the control points of the guiding device between different configurations leads to collisions, the RRT-connect algorithm [23] should be utilized in joint space to find a collision-free path in joint space. Subsequently, cubic B-spline curve fitting will be employed, and the time-optimal trajectory can be determined by solving the previously mentioned nonlinear optimization problem.

V. Experimental Results

We conducted tests and evaluations of the planning algorithm proposed in this letter within both simulated environments and real-world scenarios. The planning algorithm in this study was implemented using Python 3.10 on a desktop computer equipped with an Intel Core i7-10700 K CPU running at 3.79 GHz, 16 GB of RAM, and a 64-bit Windows 10 operating system. To verify the effectiveness of the algorithm through experimentation, we established the entire robotic system and conducted localized coverage inspection tests in a real tube sheet.

A. Results of Paired Planning

This section aims to validate the effectiveness of the pairing planning method by inspecting all heat transfer tubes within the inspection range (a total of 384 heat transfer tubes) and conducting a 50% random sampling inspection (a total of 192 heat transfer tubes), as illustrated in Fig. 6. We employed two distinct methods for paired planning and conducted a comparative analysis of the results yielded by each approach. The first method, described in Section IV(A), defines the pairing problem

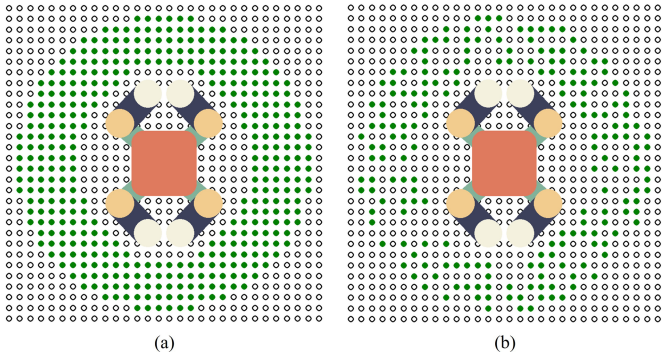

Fig. 6. All inspection and 50% sampling inspection, green dots represent the heat transfer tubes to be tested. (a) All inspection of heat transfer tubes within the inspection range; (b) 50% sampling inspection of heat transfer tubes within the inspection range.

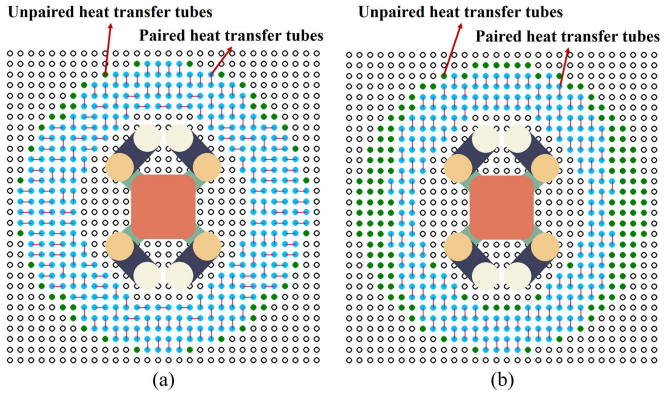

Fig. 7. Paired results under all inspection conditions. (a) 0–1 integer programming method; (b) pair by column.

as a 0–1 integer programming problem, with the optimal pairing scheme obtained through the Pulp library. The second method, commonly used in engineering, is known as pairing by column, the specific steps are outlined as follows: (1) Divide the heat transfer tubes to be inspected into multiple subsets based on the values of the horizontal coordinates (heat transfer tubes with the same horizontal coordinate are in the same column and belong to the same subset); (2) each heat transfer tube in the subset is sorted in ascending order according to the vertical coordinates; (3) in each subset, start with the first heat transfer tube to search for a heat transfer tube that can successfully pair with it (It is essential to satisfy the constraints of the inspection arm). If such a heat transfer tube exists, remove the successfully paired heat transfer tubes from the subset.

The paired results are illustrated in Figs. 7 and 8, which present the outcomes of two scenarios: an all inspection and a 50% sampling inspection. To verify the effectiveness of the algorithm in cases where there are heat transfer tubes within the inspection range that do not require inspection, or during the random sampling of heat transfer tubes in minor repair periods at nuclear power plants, we conducted the 50% sampling inspection test. In these figures, blue dots represent the heat transfer tubes that were successfully paired, whereas green dots indicate those that were not. Successfully paired heat transfer tubes are connected by red lines. We evaluate the two methods

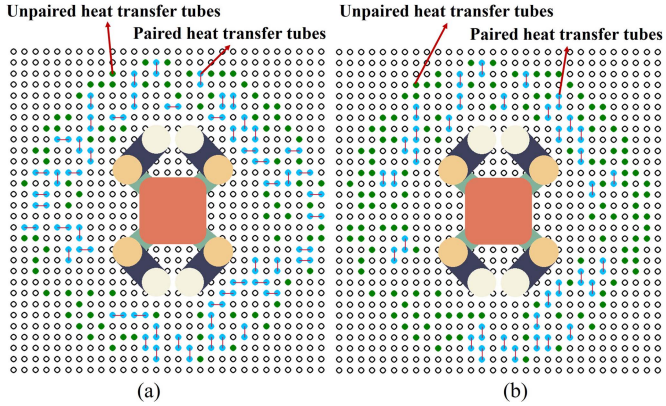

Fig. 8. Paired results under 50% sampling inspection conditions. (a) 0–1 integer programming method; (b) pair by column.

TABLE I
PAIRED RESULTS

Inspection type	Metric	0-1 integer programming	By column
All	Paired quantity	**170**	122
	Inspection time(min)	**214**	262
	Running time(s)	0.668	**0.006**
50%	Paired quantity	**55**	36
	Inspection time(min)	**137**	156
	Running time(s)	0.226	**0.003**

based on three criteria: (1) Paired quantity, (2) eddy current probe inspection time, and (3) algorithm running time. Relevant data is summarized in Table I. For the all inspection, the algorithm running time based on 0–1 integer programming generates 48 additional pairings, which may decrease the duration of the eddy-current probe inspection by over 48 minutes, accounting for approximately 18.32% of the total inspection time when using the pair by column algorithm for pairing planning. In the case of the 50% sampling inspection, the algorithm running time based on 0–1 integer programming generates 19 additional pairings, which may decrease the duration of the eddy-current probe inspection by over 19 minutes, accounting for approximately 12.18% of the total inspection time when using the pair by column algorithm for pairing planning. Thus, the pairing algorithm proposed in this letter will significantly enhance the efficiency of the eddy current probe inspection for heat transfer tubes.It is noteworthy that some heat transfer tubes that appear to meet the distance constraints of the guide tubes in Fig. 7(a), were not successfully paired. This is because, during pairing, it is also necessary to satisfy the kinematic constraints of the inspection arm, this is reflected in Formula (5).

B. Results of Inspection Sequence and Trajectory Planning

The inspection sequence and trajectory planning collaboratively determine the operational time of the inspection arm. Consequently, these two planning levels are integrated for simulation and result analysis. This study constructs a simulation environment utilizing the PyBullet simulator, by employing 0–1

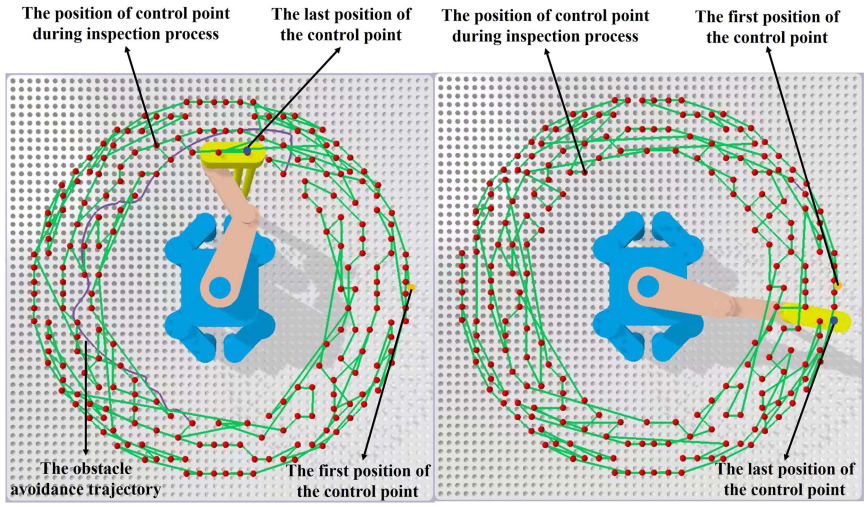

Fig. 9. Simulation results of sequential planning and trajectory planning. (a) The trajectory planning results following the use of the nearest neighbor search algorithm for sequential planning; (b) the trajectory planning results following the use of the 2-opt algorithm for sequential planning.

integer programming for the pairing of heat tubes, a quantitative comparison of two sequence planning algorithms with lower time complexity was conducted to evaluate their impacts on the operational efficiency of the inspection arm and validate the effectiveness of the time-optimal trajectory planning algorithm. In the simulation, the maximum joint angular velocity is set to 1 rd/s, the maximum angular acceleration is set to 0.5 rd/s^2, the initial angle of each joint is set to 0 rd, and the obstacle avoidance cost h in formula (7) is set to 3.

This study evaluates the inspection sequence and trajectory planning algorithms based on the following three criteria: (1) the total cost of the inspection sequence planning algorithm; (2) the running time of the inspection sequence planning algorithm; and (3) the operating time of the inspection arm. It is important to note that we do not include the trajectory planning algorithm running time in the evaluation criteria. This is because after the inspection arm moves to the required joint configuration, the eddy-current probe will conduct a 1–2 minute inspection, during which time we can plan the time-optimal trajectory for the next joint configuration.

Fig. 9 present the time-optimal trajectory planning results obtained using the nearest neighbor search algorithm and the 2-opt algorithm for sequence planning, respectively. The figures only show the positions of the control point of the guiding device, and more detailed descriptions can be found in the video materials. The total cost and the running time of the inspection sequence planning algorithm, and the inspection arm operation time are shown in Table II. The running time for the 2-opt algorithm increased by 5.84 s compared to the nearest neighbor search algorithm; however, the inspection arm operation time decreased by 39.04 s, resulting in a total time reduction of 33.20 s, accounting for approximately 6.99% of the total inspection time when using the nearest neighbor search algorithm for inspection sequence planning. Therefore, the 2-opt algorithm is more suitable for localized coverage inspection tasks in this scenario.

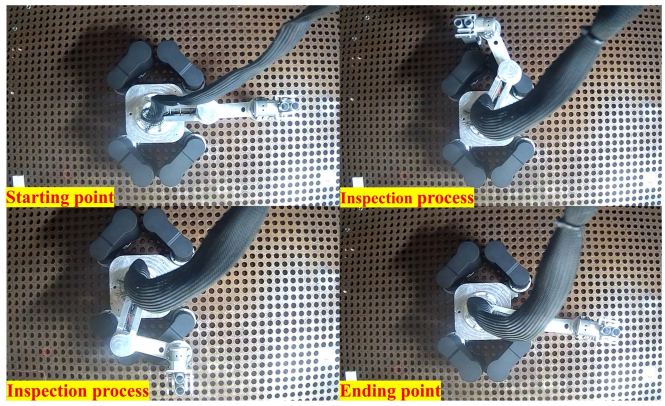

Fig. 10. Experiments on actual tube sheet.

C. Real-World Experiments

We have successfully implemented the robotic system described in this letter and verified the effectiveness of the planning algorithm in a real CPR1000 tube sheet environment. The robot was installed upside down on the tube sheet, with the maximum joint angular velocity of the inspection arm limited to 1 rd/s and the maximum angular acceleration to 0.5 rd/s^2. The planning algorithm described in this letter was employed to calculate the localized coverage inspection trajectory of the inspection arm (where the pairing planning used a 0–1 integer programming method and the sequence planning utilized the 2-opt algorithm), and the resulting trajectory was input to the joint actuators. Fig. 10 displays a screenshot of the real-world experiment. By using the planning algorithm proposed in this letter, the robot efficiently completed the localized coverage inspection task, with the operation time of the inspection arm being 437 s and no collisions occurred throughout the process. The simulation and experimental videos can be found in the video materials. In

TABLE II
RESULTS OF DIFFERENT SEQUENCE PLANNING ALGORITHMS

	Nearest neighbor search	2-opt
Total cost(rad)	77.98	**68.86**
Running time(s)	**0.44**	6.28
Operating time(s)	475.18	**436.14**

the video, the inspection arm pauses for 1 s each time it reaches the required joint configuration for inspection to demonstrate that the guiding device has reached the designated position, this duration is not included in the operating time presented in Table II.

VI. CONCLUSION

This letter proposes a novel planning framework for the SG-Climbot localized coverage inspection planning. The framework encompasses four planning levels: pairing planning, position and orientation planning for the guiding device, inspection sequence planning, and time-optimal trajectory planning. The pairing method proposed in this letter reduces the inspection time of the eddy-current probe by more than 48 minutes compared to the techniques used in engineering, which is equivalent to 18.32% of the total inspection time. It provides an effective solution for the coverage planning task of an inspection arm equipped with a dual execution device at the end. By analyzing the effects of various TSP-solving algorithms on the operational efficiency of the inspection arm, the 2-opt algorithm is chosen to address the sequential planning problem of visiting multiple nodes with shorter actual operation time, effectively ensuring the operational efficiency of the inspection arm. Simulations and experiments were conducted to validate the effectiveness of the proposed planner. The planner proposed in this letter can effectively reduce the economic losses caused by downtime maintenance in nuclear power plants.

The design of the SG-Climbot has the greatest advantage of allowing the robot to crawl within a small range while maintaining the absolute position of the guiding device unchanged. In the future, we intend to integrate this robotic characteristic with the localized coverage inspection planning algorithm presented in this letter to perform full coverage inspections of all heat transfer tubes on the tube sheet. If we can ensure that all the robot's crawling occurs during the inspection of the heat transfer tubes by the eddy current probe, the best outcome would be to inspect all heat transfer tubes on the tube sheet without requiring the time for the robot to crawl. In addition, we will attempt to integrate learning-based methods into the planning algorithm presented in this letter in the future. This will significantly enhance the efficiency of the robot's full coverage inspection.

REFERENCES

[1] Q. Z. Ye, "Safety and effective developing nuclear power to realize green and low-carbon development," *Adv. Climate Change Res.*, vol. 7, no. 1-2, pp. 10–16, 2016.
[2] X. Guo et al., "Progress in studying the fretting wear/corrosion of nuclear steam generator tubes," *Ann. Nucl. Energy*, vol. 144, 2020, Art. no. 107556.
[3] L. Obrutsky, J. Renaud, and R. Lakhan, "Overview of steam generator tube-inspection technology," *CINDE J*, vol. 35, no. 2, pp. 5–13, 2009.
[4] F. Zhao, Y. Ma, and Y. Sun, "Application and standardization trend of maintenance and inspection robot (MIR) in nuclear power station," *DEStech Trans. Eng. Technol. Res.*, 2017.
[5] L. Obrutsky, "Nuclear steam generator tube inspection tools," in *Steam Generators for Nuclear Power Plants*, Sawston, U.K.: Woodhead Publishing, 2017, pp. 495–510.
[6] Y. Seo et al., "A mobile robotic system for the inspection and repair of SG tubes in NPPs," *Int. J. Adv. Robotic Syst.*, vol. 13, no. 2, pp. 63–70, 2016.
[7] J. Li et al., "Motion planning for a quadruped robot in heat transfer tube inspection," *Automat. Construction*, vol. 168, 2024, Art. no. 105753.
[8] D. P. Arab, M. Spisser, and C. Essert, "Complete coverage path planning for wheeled agricultural robots," *J. Field Robot.*, vol. 40, no. 6, pp. 1460–1503, 2023.
[9] J. H. Zhou et al., "Research on path planning algorithm of intelligent mowing robot used in large airport lawn," in *Proc. Int. Conf. Inf. Syst. Artif. Intell.*, IEEE, 2016, pp. 375–379.
[10] C. N. Macleod et al., "Machining-based coverage path planning for automated structural inspection," *IEEE Trans. Automat. Sci. Eng.*, vol. 15, no. 1, pp. 202–213, Jan. 2016.
[11] M. D. Phung et al., "Enhanced discrete particle swarm optimization path planning for UAV vision-based surface inspection," *Automat. Construction*, vol. 81, pp. 25–33, 2017.
[12] A. K. Lakshmanan et al., "Complete coverage path planning using reinforcement learning for tetromino based cleaning and maintenance robot," *Automat. Construction*, vol. 112, 2020, Art. no. 103078.
[13] T. R. Ren et al., "Path planning for a robotic arm sand-blasting system," in *Proc. Int. Conf. Inf. Automat.*, IEEE, 2008, pp. 1067-1072.
[14] D. Leidner et al., "Robotic agents representing, reasoning, and executing wiping tasks for daily household chores," in *Auton. Agents Multi-Agent Syst.*, 2016.
[15] J. Hess, G. D. Tipaldi, and W. Burgard, "Null space optimization for effective coverage of 3D surfaces using redundant manipulators," in *Proc. IEEE/RSJ Int. Conf. Intell. Robots Syst.*, IEEE, 2012, pp. 1923–1928.
[16] D. Kaljaca, B. Vroegindeweij, and E. van Henten, "Coverage trajectory planning for a bush trimming robot arm," *J. Field Robot.*, vol. 37, no. 2, pp. 283–308, 2020.
[17] C. Zhang et al., "JPMDP: Joint base placement and multi-configuration path planning for 3D surface disinfection with a UV-C robotic system," *Robot. Auton. Syst.*, vol. 174, 2024, Art. no. 104644.
[18] J. Hogg and J. Scott, "On the use of suboptimal matchings for scaling and ordering sparse symmetric matrices," *Numer. Linear Algebra with Appl.*, vol. 22, no. 4, pp. 648–663, 2015.
[19] R. Rajaby and W. K. Sung, "Computing asymmetric median tree of two trees via better bipartite matching algorithm," in *Proc. Int. WorkShop Combinatorial Algorithms*, Cham: Springer, 2017, pp. 356–367.
[20] O. Mersmann et al., "Local search and the traveling salesman problem: A feature-based characterization of problem hardness," in *Proc. Learn. Intell. Optimization, 6th Int. Conf.*, Paris, France, Revised Selected Letters, Springer Berlin Heidelberg, 2012, pp. 115–129.
[21] K. Helsgaun, "An effective implementation of the Lin–Kernighan traveling salesman heuristic," *Eur. J. Oper. Res.*, vol. 126, no. 1, pp. 106–130, 2000.
[22] J. J. Kuffner and S. M. LaValle, "RRT-connect: An efficient approach to single-query path planning," in *Proc. ICRA. Millennium Conf. IEEE Int. Conf. Robot. Autom.. Symposia Proc.*, IEEE, 2000, vol. 2, pp. 995–1001.
[23] P. Virtanen et al., "SciPy 1.0: Fundamental algorithms for scientific computing in python," *Nature Methods*, vol. 17, no. 3, pp. 261–272, 2020.